



# Babassu mesocarp (*Orbignya phalerata* Mart) nanoparticle-based biosensors for indirect sulfite detection in industrial juices

Ana Siqueira Siqueira do Nascimento Marreiro Teixeira<sup>1,2</sup> · Paulo Ronaldo Sousa Teixeira<sup>2</sup> · Emanuel Airton de Oliveira Farias<sup>3</sup> · Brandon Ferraz e Sousa<sup>4</sup> · Kátia Bonfim de Leite Moura Sérvulo<sup>4</sup> · Durcilene Alves da Silva<sup>3</sup> · Carla Eiras<sup>1</sup>

Received: 27 October 2019 / Revised: 17 February 2020 / Accepted: 8 March 2020 / Published online: 29 April 2020  
© Springer-Verlag GmbH Germany, part of Springer Nature 2020

## Abstract

The present work proposes a new electrochemical sulfite biosensor based on babassu mesocarp nanoparticles (BMNPs) immobilized on the surface of a pyrolytic graphite electrode (PGE). The synthesized nanoparticles had a size of 121.5 nm and a zeta potential of  $-28.1$  mV and were used as a support for the immobilization of chitosan (CHIT) and polyphenol oxidase (PPO) obtained from sweet potatoes (*Ipomea batatas* (L.)). The electrochemical activity of the PGE/BMNPs/CHIT/GA/PPO biosensor was measured using cyclic voltammetry (CV) and square wave voltammetry (SWV), and the biosensor was shown to have a sensitivity of  $2.18 \mu\text{A}/\mu\text{mol L}^{-1}$ , a detection limit of  $0.151 \mu\text{mol L}^{-1}$ , and quantitation limit of  $0.452 \mu\text{mol L}^{-1}$  for sulfite. The principle of analysis for the developed biosensor is based on the inhibitory effect of sulfite on the activity of the PPO enzyme. This biosensor was successfully employed for the analysis of industrial juice, without the need to pre-treat the sample.

**Keywords** Enzymatic biosensor · Polyphenol oxidase · Sulfite detection · Polymeric nanoparticles · Electrochemical biosensor

## Introduction

Food additives are natural or synthetic substances added to foods to render them with a particular technological or sensory function, for example, to combat bacterial degradation, restore color, or add flavor [1].

These can be primarily divided into 6 groups, namely preservatives, nutritional additives, dyes, flavoring agents,

texturizing agents, and diversified agents. Preservatives can be further subdivided into antimicrobials, antioxidants, and anti-bleaching agents [2].

Sulfite or sulfite agents such as sulfur dioxide ( $\text{SO}_2$ ), sodium sulfite ( $\text{Na}_2\text{SO}_3$ ), potassium sulfite ( $\text{K}_2\text{SO}_3$ ), sodium bisulfite ( $\text{NaHSO}_3$ ), potassium bisulfite ( $\text{KHSO}_3$ ), sodium metabisulfite ( $\text{Na}_2\text{S}_2\text{O}_5$ ), and potassium metabisulfite ( $\text{K}_2\text{S}_2\text{O}_5$ ) can act as preservatives [3, 4]. These additives are used to improve the food aroma, lighten and stabilize food products, and prevent fermentation, and as antimicrobial agents [5, 6]. They are widely used in foods such as wines, processed juices, dried fruit, dehydrated biscuits, and fish [7, 8].

Despite their effectiveness in food preservation, sulfites reportedly cause numerous adverse reactions on human health. Studies have shown that extensive ingestion of this additive induces harmful effects on cells and tissues, causing life-threatening asthma attacks and allergic reactions [9, 10]. Symptoms of dermatitis, hives, flushing, hypotension, abdominal pain, and diarrhea have also been reported [11, 12].

Therefore, there is a need to monitor sulfite levels in processed foods and beverages, in order to maintain compliance with the regulatory guidelines proposed by current legislation. The Food and Drug Administration (FDA, USA) recommends the use of warning labels on any food product

**Electronic supplementary material** The online version of this article (<https://doi.org/10.1007/s10008-020-04546-w>) contains supplementary material, which is available to authorized users.

✉ Carla Eiras  
carla.eiras.ufpi@gmail.com

- <sup>1</sup> Laboratório de Pesquisa e Desenvolvimento de Novos Materiais e Sensores MatSens, CT, UFPI, Campus Ministro Petrônio Portela, Teresina, PI 64049-550, Brazil
- <sup>2</sup> Instituto Federal de Educação Ciência e Tecnologia do Piauí – IFPI, Teresina, PI 64018-900, Brazil
- <sup>3</sup> Núcleo de Pesquisa em Biodiversidade e Biotecnologia, BIOTEC, Universidade Federal do Delta do Parnaíba (UFDPA), Parnaíba, PI 64202-020, Brazil
- <sup>4</sup> Departamento de Bioquímica e Farmacologia, Universidade Federal do Piauí, Teresina, PI 64049-550, Brazil

containing more than 10 mg/kg sulfite, or a beverage containing more than 10 mg/L sulfite [13].

A number of techniques have been developed for the quantitative analysis of sulfite, such as titration [14], chromatography [15], capillary electrophoresis [16, 17], flow injection analysis [18, 19], and fluorescence spectroscopy [20, 21]. However, some of these techniques are time-consuming while others require sample pretreatment or high cost.

Biosensors are believed to be a viable alternative for the rapid detection and quantification of sulfites in food products, since they are simple, low-cost devices with high sensitivity and stability, and a short analysis time [22–24].

Enzymatic biosensors are constructed by immobilizing enzymes on the surface of the electrode and have aroused interest due to their increased selectivity and stability [25, 26].

The enzyme particularly used in the construction of biosensors is polyphenol oxidase (PPO), also known as tyrosinase or catechol oxidase. This enzyme is a natural oxidoreductase, with two copper atoms at its active center, catalyzing oxidation reactions including the hydroxylation of monophenols to o-diphenols and the subsequent oxidation of diphenols to o-quinones in the presence of molecular oxygen [27–29].

Nanoparticles are other materials widely used in the construction of biosensors. They have advantageous properties such as high surface area and low diffusional limitation, which provide an adequate environment for the immobilization of the enzymes, while maintaining their bioactivity and facilitating the transfer of electrons between the redox center and the electrode surface [30–32].

Polymeric nanoparticles used in the present work were developed using the natural polymer from babassu mesocarp (BM) (*Orbignya phalerata* Mart). BM is the substance harvested from between the babassu coconut epicarp and endocarp [33]. It is a useful material with no toxicity and is widely used as a binder. These characteristics allow it to be used for different industrial and health applications [34, 35].

The present work was aimed at the construction of an electrochemical biosensor for the indirect determination of sulfite in industrial juices, using a pyrolytic graphite carbon electrode modified with polymeric babassu mesocarp nanoparticles, polyphenol oxidase enzyme, chitosan, and glutaraldehyde for the construction of the active layer.

## Materials and methods

### Materials and reagents

The following reagents were used in this study: dimethylsulfoxide (DMSO) (Sigma-Aldrich), polyvinylpyrrolidone (PVP) (Sigma-Aldrich), catechol ( $C_6H_6O_2$ ) (Sigma-Aldrich), chitosan-GD = 85% (Sigma-Aldrich), glutaraldehyde (GA) (Vetec) 50% (v/v), sodium phosphate monobasic

( $NaH_2PO_4$ ) (Sigma-Aldrich), and sodium phosphate dibasic ( $Na_2H_2PO_4$ ) (Sigma-Aldrich). All reagents were of analytical standards and did not require prior purification. Ascorbic acid (Dinamica, Brazil), potassium sorbate (Dinamica, Brazil), and sucrose (Dinamica, Brazil) of analytical standards were used for the interference studies.

The  $0.5\text{ g L}^{-1}$  BM stock solution was prepared in DMSO, while the stock solutions of catechol ( $0.05\text{ mol L}^{-1}$  and  $0.001\text{ mol L}^{-1}$ ) and sulfite  $0.1\text{ mol L}^{-1}$  were prepared fresh in  $0.1\text{ mol L}^{-1}$  phosphate buffer solution (pH 7.2), obtained using  $NaH_2PO_4$  and  $Na_2H_2PO_4$ . The  $0.1\text{ mol L}^{-1}$  (pH 7.2) phosphate buffer was also used as a supporting electrolyte in all electrochemical measurements with the biosensor. Chitosan was prepared at  $1.0\text{ g L}^{-1}$  in 1% (v/v) acetic acid using ultrapure water. Glutaraldehyde solution (2.5% (v/v)) was prepared in  $0.1\text{ mol L}^{-1}$  phosphate buffer (pH 7.2).

Babassu mesocarp coconut *in natura* was acquired in powder form from the Department of Agrarian Sciences of the Federal University of Piauí (Brazil), followed by granulometry to screen for grain size selection, which was determined to be approximately 0.074 mm. The sweet potatoes (*Ipomoea batatas* (L.) (Lam.)) and the industrialized juice samples were purchased locally from the Teresina-Pi city.

### Synthesis of BMNPs

BMNPs were prepared by the dialysis method in which the polymer was dissolved in an organic solvent and added to a dialysis membrane, where the formation of nanoparticles is based on the gradual exchange of the organic solvent with water [36]. BM was dissolved in DMSO to a final concentration of  $0.50\text{ g L}^{-1}$ . The solution was maintained under stirring conditions of 500 rpm at a temperature of  $50\text{ }^\circ\text{C}$  for 1 h in an ultrasonic bath for the total dilution of BM.

The BM solution prepared in DMSO was then placed on a 76-mm-thick dialysis membrane with a 12-kDa exclusion limit, for dialysis in ultrapure water for 72 h. During this period, the dialysis water was changed every 12 h. UV-Vis spectroscopy was used to monitor the presence of DMSO during dialysis.

Finally, the BMNP dispersion was filtered using a  $0.45\text{-}\mu\text{m}$  aperture filter to remove the precipitates, and the filtrate reserved for further analysis. The pH of the BMNPs was determined to be 8.5, using a HI 2221 Hanna pH meter.

### Dynamic light scattering and zeta potential

Dynamic light scattering (DLS) and zeta potential analyses were performed using a Zetasizer Nano-ZS90-Malvern in order to determine the mean size and charge of BMNPs. The hydrodynamic diameter was measured by DLS using a 633-nm laser with a fixed dispersion angle of  $173^\circ$ . DLS analysis was performed in triplicate at a temperature of  $25\text{ }^\circ\text{C}$ .

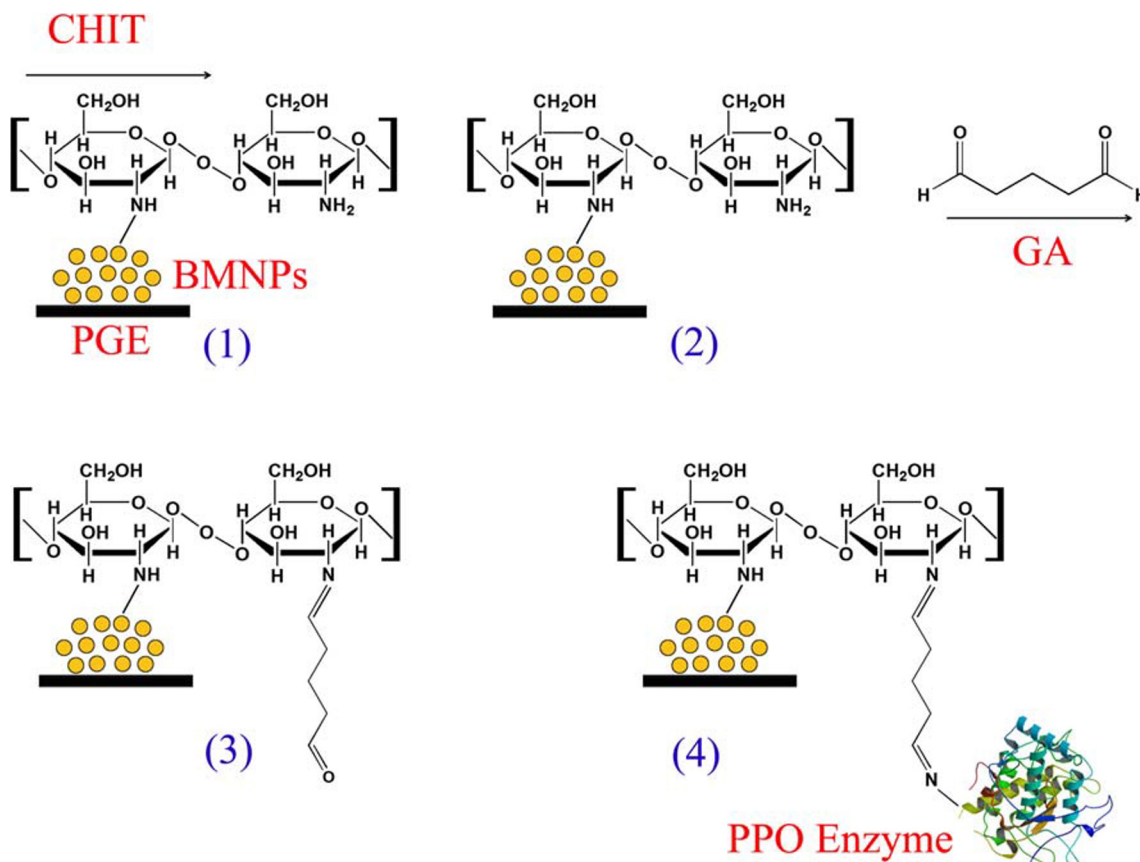


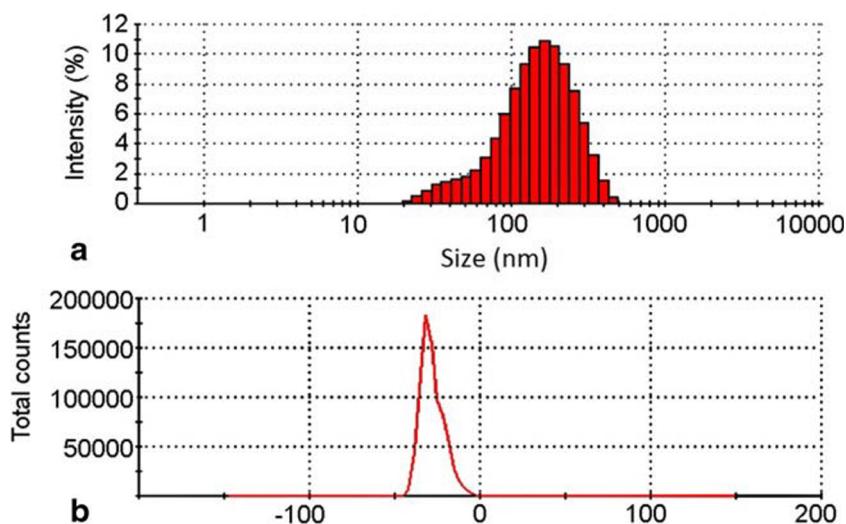
**Fig. 1** Schematic illustration of the different steps for construction of a sulfite biosensor. (1) CHIT binds to BMNPs through electrostatic interactions; (2) amine-aldehyde bond between CHIT and GA; (3)

aldehyde-amine bond between GA and PPO enzyme; (4) the PGE/BMNPs/CHIT/GA/PPO biosensor obtained

**Scanning electron microscopy**

The morphology of the BMNPs was recorded by a FEI Quanta FEG 250 scanning electron microscope. To prepare the SEM (scanning electron microscopy) sample, 50  $\mu$ L of the MBNPs suspension was deposited on a substrate coated with aluminum foil, and the sample was then dried and coated with gold.

**Fig. 2** (a) Size distribution and (b) zeta potential of BMNPs synthesized by dialysis



**Preparation of the crude enzymatic extract**

The PPO enzyme was obtained from sweet potatoes (*Ipomoea batatas* (L.) (Lam.)), using the crude extract as the enzymatic source. The sweet potatoes were washed in running water, peeled, and cut into small pieces to facilitate homogenization. Subsequently, 25 g potatoes was crushed using a blender in

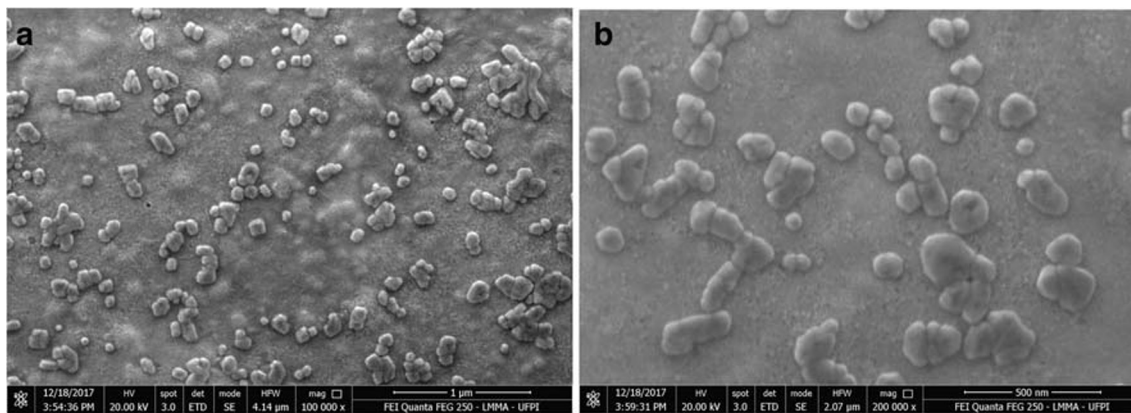


**Fig. 3** SEM images of BMNPs obtained at (a)  $\times 100,000$  and (b)  $\times 200,000$

100 mL of ice-cold phosphate buffer (at  $0.1 \text{ mol L}^{-1}$ , pH 7.2) and 2.5 g PVP for 2 min.

The mixture was then filtered and centrifuged using a Sigma 2K15 bench centrifuge at 15,000 rpm for 30 min at  $4^\circ\text{C}$ . The supernatant was then stored at  $4^\circ\text{C}$  and used as the enzymatic source of PPO for the determination of enzymatic activity and concentration of total soluble proteins.

#### Determination of PPO activity in the crude extract

The PPO activity in the crude enzymatic extract was determined by mixing 0.2 mL of the enzymatic extract with 2.8 mL of  $0.05 \text{ mol L}^{-1}$  catechol as substrate (prepared at  $0.1 \text{ mol L}^{-1}$  phosphate buffer solution, pH 7.2 at  $25^\circ\text{C}$ ). The absorbance of o-quinone (reaction product) was measured on a Cary 60 UV-visible spectrophotometer (Agilent Technologies) using a quartz cuvette with an optical path of 1.0 cm at a  $\lambda$  of 410 nm after 2 min of reaction. One activity unit (Eq. 1) is defined as the amount of enzyme which increases 0.001 units of absorbance per minute, under the conditions mentioned above [37, 38].

$$a = \frac{\Delta A \times 60 \times 1000}{\Delta t \times d \times \text{Vol (sample)}} \quad (1)$$

where  $a$  is the unit of PPO activity per mL;  $\Delta A$  is the change in absorbance;  $\Delta t$  is the reaction time variation (min);  $d$  is the cuvette diameter; and Vol (sample) is the sample volume (mL).

#### Determination of total soluble proteins in the crude extract

The concentration of total proteins was determined in triplicates using the methodology described by Bradford [39]. Bovine serum albumin was used as the standard.

#### Preparation of PGE/BMNPs/CHIT/GA/PPO biosensor

The pyrolytic graphite electrode (PGE) was used as the working electrode. In order to obtain a clean surface capable of

good adsorption of the materials, the PGE was first polished before modification with a thicker metallographic abrasive paper (sandpaper 200), and then with a finer metallographic abrasive paper (sandpaper 1200). The electrode was then washed with ultrapure water and sonicated for 5 min in isopropyl alcohol, followed by ultrapure water for the same time interval. PGE was then dried at room temperature ( $24^\circ\text{C}$ ) to complete the cleaning process.

The cleaning efficiency was evaluated by cyclic voltammetry. Clean PGE was introduced into the electrochemical cell and successive scans were applied in the potential range of  $-0.1$  to  $+1.5 \text{ V}$  vs the saturated calomel electrode (SCE) in  $1.0 \text{ mol L}^{-1} \text{ H}_2\text{SO}_4$  at  $100 \text{ mV s}^{-1}$ . The surface was considered clean when the voltammogram did not show any electrochemical process.

PGE was modified after cleaning through the deposition of multilayer casting films, beginning with the deposition of  $50 \mu\text{L}$  BMNP dispersion on the clean electrode surface, followed by drying at room temperature for 2 h.

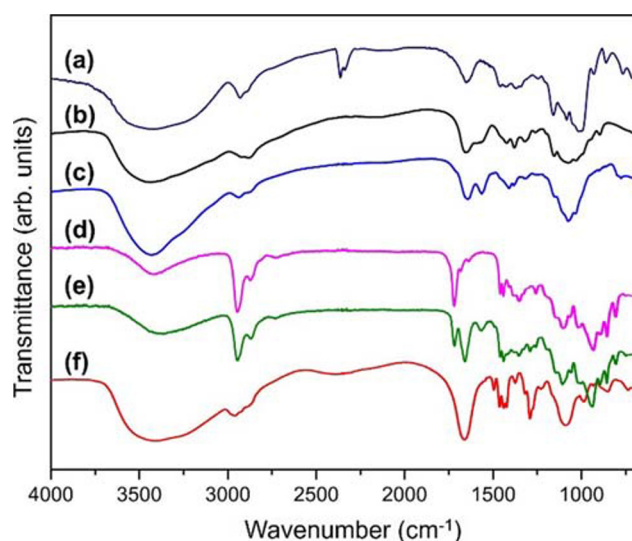
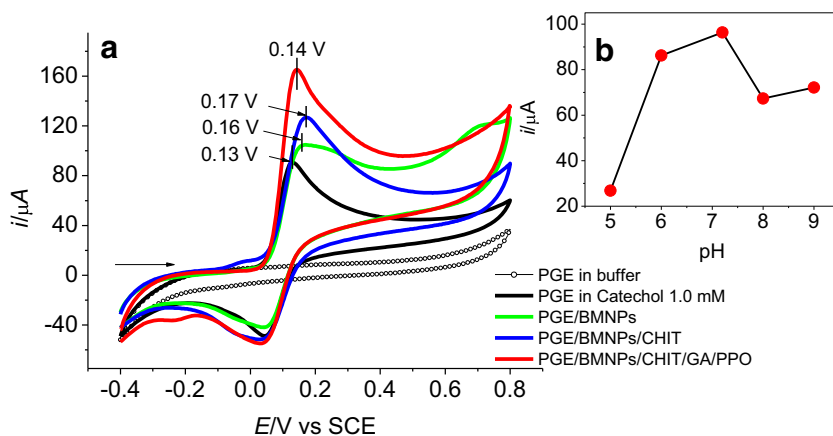


**Fig. 4** FTIR spectra obtained from biosensor layers: (a) BMNPs, (b) CHIT, (c) BMNPs/CHIT, (d) BMNPs/CHIT/GA, (e) BMNPs/CHIT/GA/PPO, (f) PPO

**Fig. 5** (a) Cyclic voltammograms obtained for PGE, PGE/BMNPs, PGE/BMNPs/CHIT, and PGE/BMNPs/CHIT/GA/PPO recorded in 1.0 mmol L<sup>-1</sup> catechol solubilized in 0.1 mol L<sup>-1</sup> phosphate buffer. (b) Electrolyte pH effect on the catechol oxidation peak current for PGE/BMNPs/CHIT/GA/PPO. All measurements were obtained with  $v = 10 \text{ mV s}^{-1}$



Subsequently, 50  $\mu\text{L}$  of 1.0 g L<sup>-1</sup> CHIT solution was deposited on the electrode, previously modified with BMNPs, and dried at room temperature for 2 h. Then, 50  $\mu\text{L}$  of 2.5% (v/v) GA solution was added onto the surface of the electrode already modified with BMNPs/CHIT and dried for 2 h at room temperature. The electrode was carefully washed after drying with 0.1 mol L<sup>-1</sup> phosphate buffer solution (pH 7.2) to remove excess cross-linking agent.

Finally, 50  $\mu\text{L}$  of PPO was immobilized as the last layer of the electrode and dried under refrigeration ( $\cong 4 \text{ }^\circ\text{C}$ ) for 6 h. The PGE/BMNPs/CHIT/GA/PPO biosensor was stored in a volumetric flask containing a 0.1 mol L<sup>-1</sup> phosphate buffer solution under refrigeration.

In the film deposition process to construct the PGE/BMNPs/CHIT/GA/PPO biosensor (Fig. 1), the anionic BMNPs bind to the cationic CHIT through electrostatic interactions between opposite charges. The amino groups on CHIT as well as those in the PPO enzyme bind to terminal aldehyde groups of the GA cross-linking agent, through covalent bonds. These cross-linking

covalent bonds between the amine groups confer stability during variations in pH and ionic strength of the solution [40].

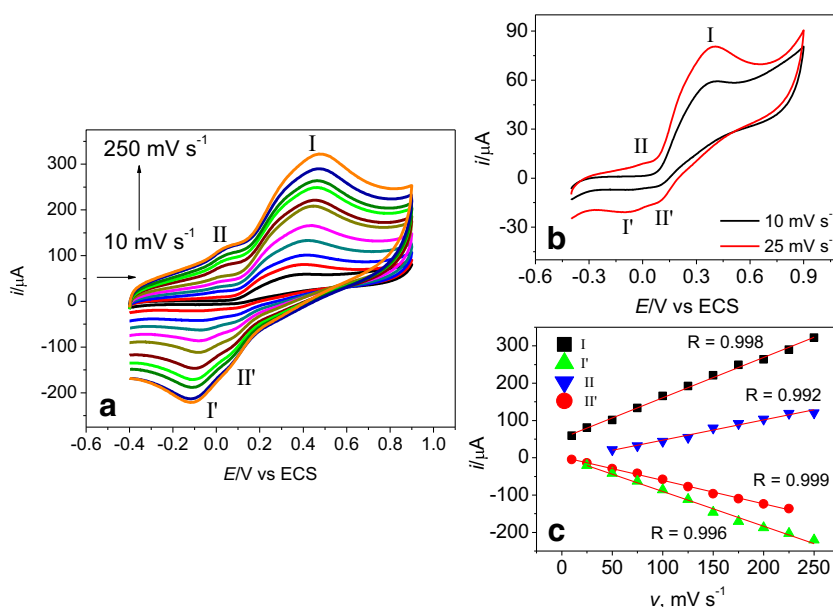
### Biosensor layers Fourier transform infrared spectroscopy

In order to identify the interactions between the biosensor layers, Fourier transform infrared spectroscopy (FTIR) analyses were performed on KBr pellets. The spectra were obtained in Paragon 1000 equipment, Perkin-Elmer, USA, in the wavelength range between 4000 and 400  $\text{cm}^{-1}$  during 64 scans, with a resolution of 2  $\text{cm}^{-1}$ .

### Electrochemical measurements

The electrochemical measurements were performed using cyclic voltammetry (VC) and square wave voltammetry (VOQ) with a METROHM's Dropsens  $\mu\text{Stat}$  400 bipotentiostat/galvanostat which was used an electrochemical cell with three

**Fig. 6** (a) Cyclic voltammograms obtained at different scanning rates: 10, 25, 50, 75, 100, 125, 150, 175, 200, 225, and 250  $\text{mV s}^{-1}$ . (b) Voltammograms comparing the PGE/BMNPs/CHIT/GA/PPO response at 10 and 25  $\text{mV s}^{-1}$ . (c) Influence of the scan rate on the peak current values for the oxidation processes I and II and for the reduction processes I' and II' of the PGE/BMNPs/CHIT/GA/PPO biosensor. All voltammograms were recorded in 1.0 mmol L<sup>-1</sup> catechol solubilized in 0.1 mol L<sup>-1</sup> phosphate buffer, pH 7.2



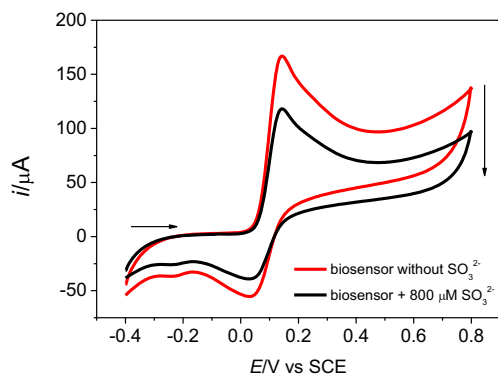


**Fig. 7** Cyclic voltammograms obtained for the PGE/BMNPs/CHIT/GA/PPO biosensor (a) in the absence and (b) in the presence of sulfite at  $800 \mu\text{mol L}^{-1}$ . The voltammograms were obtained in  $1.0 \text{ mmol L}^{-1}$  catechol solution solubilized in  $0.1 \text{ mol L}^{-1}$  phosphate buffer, pH 7.2, and  $\nu = 10 \text{ mV s}^{-1}$

electrodes, the saturated calomel electrode (SCE) as the reference electrode, a platinum auxiliary electrode ( $A = 2.0 \text{ cm}^2$ ), and a PGE as the working electrode.

### Interfering test

The study of potential interferences was performed by square wave voltammetry using ascorbic acid, potassium sorbate, and sucrose, in  $1.0 \text{ mmol L}^{-1}$  catechol solubilized in  $0.1 \text{ mol L}^{-1}$  phosphate buffer (pH 7.2). Initially,  $60 \mu\text{mol L}^{-1}$  of sulfite was added to the electrochemical cell. The impact of the increase in concentration of each possible interferent on the analytical response obtained for the sulfite was then measured.

### Indirect determination of sulfite in industrialized juice samples

Industrial juice samples were used without pretreatment, and  $4.0 \text{ mL}$  of each sample was added directly to the electrochemical cell containing  $16.0 \text{ mL}$  of  $1.0 \text{ mmol L}^{-1}$  catechol solution in  $0.1 \text{ mol L}^{-1}$  phosphate buffer (pH 7.2). The square wave voltammograms were obtained in triplicate by the standard addition method.

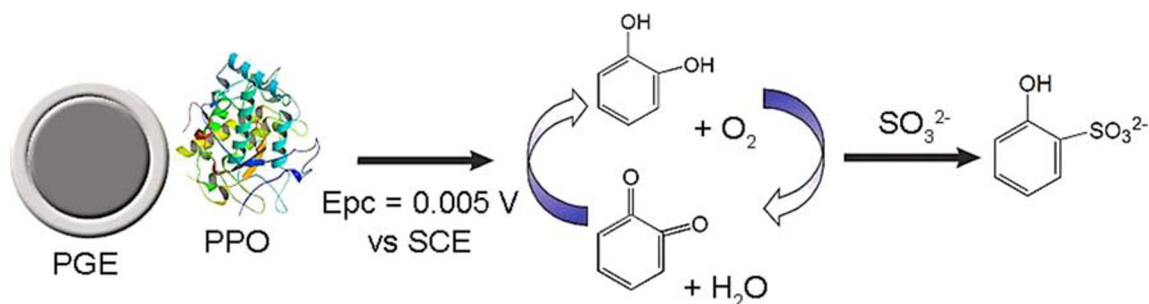


**Fig. 8** Schematic representation of the inhibition of oxidation of catechol to o-quinone in the presence of sulfite

## Results and discussion

### Characterization of BMNPs

The size distribution and zeta potential of BMNPs obtained by dialysis are shown in Fig. 2. Figure 2a shows that the average particle size was found to be  $121.5 \text{ nm}$ . This result corroborates with that of Quintanar-Guerrero et al. [41], who found that polymer nanoparticles often had a size between  $100$  and  $500 \text{ nm}$ .

The polydispersity index (PDI) provides information about the degree of sample homogeneity. PDI is indirectly proportional to the homogeneity of the particle diameter present in sample [42]. The PDI obtained for BMNPs was  $0.254$ , which indicates that the system has low polydispersity, i.e., it has good particle size distribution.

Zeta potential analysis of BMNPs showed a value of  $-28.1 \text{ mV}$  (Fig. 2b). According to Patel and Agrawal [43], samples with zeta potential values between  $\pm 20 \text{ mV}$  and  $\pm 30 \text{ mV}$  are moderately stable, showing little tendency towards flocculation. The negative zeta potential of BMNPs is due to the anionic characteristics of the babassu mesocarp [33].

The colloidal stability of BMNPs was monitored for 6 months and it was observed that the colloidal dispersion remained stable without significant changes in particle size, which may be associated with the zeta potential observed for this sample.

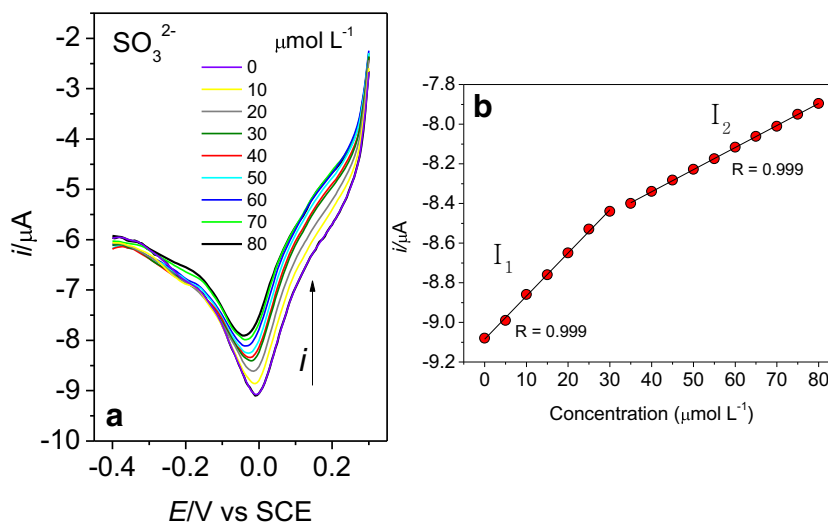
The morphology of BMNPs was evaluated by scanning electron microscopy (SEM) (Fig. 3 a and b). SEM images for the BMNPs show irregular-shaped particles with an average size of  $89.3 \text{ nm}$ .

The mean diameter values of BMNPs as observed in SEM were lower than those observed in DLS. This was expected since the samples are solvated for DLS analysis while they are dried in ultra-high vacuum (UHV) for SEM samples analysis [44]. DLS measures the hydrodynamic radius of the dispersed particles while SEM provides the projected surface area based on the amount of incident electrons transmitted through the sample [45].

### Enzymatic activity and total protein concentration

Specific activity and total protein concentration were evaluated using the crude extract obtained from sweet potatoes

**Fig. 9** (a) Square wave voltammograms (SWV) (amp. 10 mV, freq. 20 Hz, and eq time 10 s) obtained from PGE/BMNPs/CHIT/GA/PPO biosensor in 1.0 mM catechol solubilized in 0.1 M phosphate buffer (pH 7.2) in the presence of different sulfite concentrations and (b) the analytical curve obtained



(*Ipomoea batatas* (L.) (Lam.)). The PPO activity and total protein concentration were estimated to be 2300 U mL<sup>-1</sup> and 0.46 mg mL<sup>-1</sup>, respectively.

Sartori et al. [46] found enzymatic activity and total protein concentration to be 1305 U mL<sup>-1</sup> and 0.44 mg mL<sup>-1</sup> respectively, from the same amount of sweet potato plant tissue and PVP protective agent.

**Biosensor layers Fourier transform infrared spectroscopy**

The characteristic bands of the groups presenting the biosensor construction steps are represented in Fig. 4.

The band observed at 3425 cm<sup>-1</sup> in BMNPs (a), CHIT (b), and PPO (f) is related to the stretch (OH) present in alcohols [47]. This band appears overlapping the stretch band (-NH<sub>2</sub>) in CHIT (b) and PPO (f) [48]. It is noticed that when BMNPs are immobilized on the surface of CHIT (c), there is an increase in the intensity of this band, suggesting the interaction between the groups (OH) of the BMNPs with the groups (-NH<sub>2</sub>) of the CHIT.

The band at 1729 cm<sup>-1</sup> in steps (d) and (e) is related to GA free aldehyde (-COH) groups [49, 50]. It is noticed that when the PFO enzyme is added to the BMNPs/CHIT/GA system, there is a considerable decrease of this band, suggesting that there was a cross-

linking process, where GA (-COH) groups bind to the groups (-NH<sub>2</sub>) of CHIT and PPO.

The band observed at 1100 cm<sup>-1</sup> in steps (b) to (f) corresponds to aliphatic amines [51]. It is noticed that in the GA cross-linked samples, (d) and (e), the intensity of this band is decreased, indicating that these groups were linked to the GA groups, forming an imine bond (N=C).

**Electrochemical behavior of catechol in the presence of the PGE/BMNPs/CHIT/GA/PPO biosensor**

Figure 5a shows the cyclic voltammograms obtained for PGE, PGE/BMNPs, PGE/BMNPs/CHIT, and PGE/BMNPs/CHIT/GA/PPO in the presence of catechol. Figure 5b shows the electrolytic pH effect on the anodic peak current of the PGE/BMNPs/CHIT/GA/PPO biosensor.

Unmodified ECP in the presence of the catechol exhibits an oxidation process of 0.13 V vs SCE, and the oxidation product, o-quinone, the reduction process in 0.05 V vs SCE (black curve) [46].

When BMNPs were immobilized on PGE (Fig. 5a, green curve), an enhancement in the catechol peak oxidation process was observed, as well as an increase in the current values. These changes in the catechol electrochemical behavior on the PGE/BMNPs surface confirmed the immobilization of the BMNPs.

The immobilization of the CHIT layer forming the PGE/BMNPs/CHIT system (blue curve) restored the peak shape of the catechol redox processes, further increasing its current values from 104 to 127 μA (Fig. 5a). This behavior probably occurs due to the positive charges of the chitosan, which facilitate the reaction with the catechol on the electrode surface.

Finally, immobilization of PPO forming PGE/BMNPs/CHIT/GA/PPO biosensor increased the current in the catechol redox processes (red curve) by 181.91% compared with that with only

**Table 1** Characteristics of the calibration curve for sulfite using PGE/BMNPs/CHIT/GA/PPO biosensor

	LOD (μM)	LOQ (μM)	Slope	Analytical sensitivity (μA/μM)
I <sub>1</sub>	0.151	0.452	0.218	2.18
I <sub>2</sub>			0.112	1.12

**Table 2** Comparison of the analytical parameters obtained using different biosensors for sulfite determination

Electrochemical technique used	Electrode**	Linear range ( $\mu\text{M}$ )	LOD $\mu\text{M}$	Reference
CV	E Au/PPY/PBNPs/SOx <sup>I</sup>	0.5–1000	0.1	[60]
DPV	GCE/AuNPs-MWCNTs-PAH/PPO <sup>II</sup>	0.5–22	0.4	[46]
CV	EPt/PPY/SOx <sup>III</sup>	0.9–400	0.9	[61]
CV	E Au/CytC/SDH <sup>IV</sup>	0.5–5.5	0.000044	[62]
CV	EIT/CytC/SOx <sup>V</sup>	40–5900	40.0	[63]
SWV	GPE/IL/BF <sup>VI</sup>	0.05–250	0.02	[64]
CV	E Au/GNPs@Fe <sub>3</sub> O <sub>4</sub> /SOx <sup>VII</sup>	0.50–1000	0.15	[23]
CV	E Au/PANI/cMWCNT/CHIT/AuNPs/SOx <sup>VIII</sup>	0.75–400	0.5	[65]
SWV	PGE/BMNP/CHIT/GA/PPO <sup>IX</sup>	5–80	0.15	This work

CV, cyclic voltammetry; SWV, square wave voltammetry; DPV, differential pulse voltammetry

<sup>I</sup> E Au/PPY/PBNPs/SOx: polypyrrole-modified gold electrode, Prussian blue nanoparticles, and sulfite oxidase enzyme; <sup>II</sup> GCE/AuNPs-MWCNTs-PAH/PPO: glass carbon electrode modified with gold nanoparticles, carbon nanotubes, hydrochloride polyallylamine, and the enzyme polyphenol oxidase; <sup>III</sup> EPt/PPY/SOx: platinum electrode modified with polypyrrole and the enzyme sulfite oxidase; <sup>IV</sup> E Au/CytC/SDH: gold electrode modified with cytochrome C and the enzyme sulfite dehydrogenase; <sup>V</sup> SPE/CytC/SOx: screen-printed electrode modified with cytochrome C and the enzyme sulfite oxidase; <sup>VI</sup> GPE/IL/BF: graphene nanosheet paste electrode modified with ionic liquid and benzoyl ferrocene; <sup>VII</sup> E Au/GNPs@Fe<sub>3</sub>O<sub>4</sub>/SOx: modified gold electrode with carboxylated sheets, magnetic nanoparticles, and the enzyme sulfite oxidase; <sup>VIII</sup> E Au/PANI/cMWCNT/CHIT/AuNPs/SOx: polyaniline-modified gold electrode, multilayer revised carbon nanotube, chitosan, gold nanoparticle, and the sulfite oxidase enzyme; <sup>IX</sup> PGE/MBNPs/CHIT/GA/PPO: pyrolytic graphite electrode modified with babassu mesocarp nanoparticles, chitosan, glutaraldehyde, and the polyphenol oxidase enzyme (produced in this work)

PGE (black curve). This current increase after PPO immobilization indicated catalytic effect of the enzyme during the redox reactions of the catechol on the surface of this biosensor.

### pH effect

pH is an important parameter in the determination of enzymatic activity, directly influencing the analytical response of the biosensor. Using a new PGE/BMNP/CHIT/GA/PPO biosensor, the influence of electrolytic pH in the range of pH 5.0 to 9.0 in 1.0 mmol L<sup>-1</sup> catechol in phosphate buffer 0.1 mol L<sup>-1</sup> was investigated solubilized (Fig. 5b).

Figure 5b shows the effect of pH on the anodic peak current. The PPO activity is seen to be effectively inhibited in acidic medium [52], where at pH 5.0 the biosensor had a current of 26.81  $\mu\text{A}$ . When pH was increased to 6.0, an increase in the electrode surface reactivity was observed, with an increment in current to 86.25  $\mu\text{A}$ , which occurs due to the decrease in the concentration of H<sup>+</sup> ions [53]. The optimum pH for this biosensor was 7.2, with a current of 96.37  $\mu\text{A}$ . Therefore, this pH was selected for subsequent studies. At alkaline pH (pH 8 and 9), there was a decrease in biosensor activity, with a decrease in current to 67.34  $\mu\text{A}$  and 56.16  $\mu\text{A}$ , respectively. This result may be related to the possible inactivation of the enzyme at higher pH values [54].

**Fig. 10** Square wave voltammograms (amp. 10 mV, freq. 20 Hz, and eq time 10 s) obtained in the presence of different concentrations of (a) potassium sorbate, (b) sucrose, and (c) ascorbic acid. All voltammograms were obtained using the PGE/MBNPs/CHIT/GA/PPO biosensor in 1.0 mM catechol solubilized in 0.1 M phosphate buffer, pH 7.2

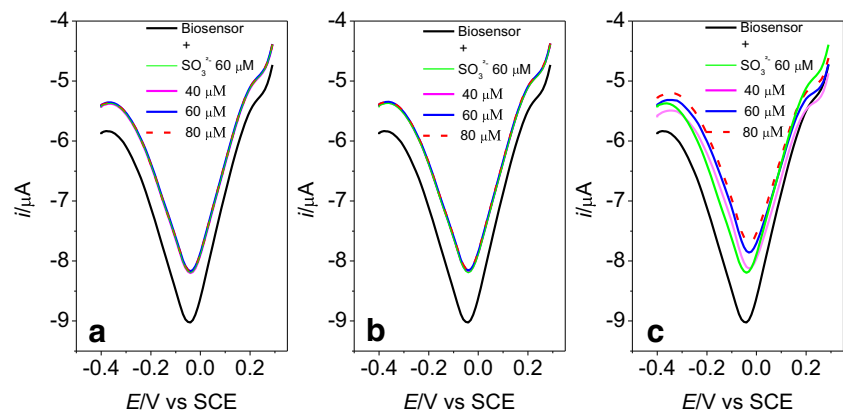




**Table 3** Sulfite recovery in previously enriched commercial juice samples

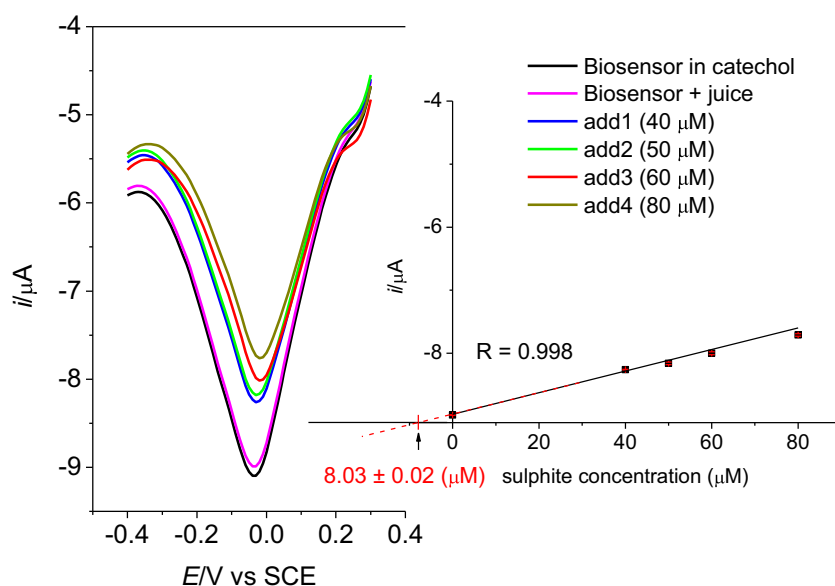
Added ( $\mu\text{M}$ )	Recovery ( $\mu\text{M}$ )	Recovery (%)
5.0	$5.47 \pm 0.02$	109.40
10.0	$10.12 \pm 0.01$	101.20
20.0	$19.22 \pm 0.03$	96.10
40.0	$37.88 \pm 0.02$	94.70

### Scan rate and electrochemical mechanism

The effect of scanning speed on the electrochemical response of the PGE/BMNPs/CHIT/GA/PPO biosensor was evaluated by varying the scanning rates during catechol oxidation. Cyclic voltammograms were obtained at scanning rates ranging from 10 to 250  $\text{mV s}^{-1}$  (Fig. 6a).

It is observed in Fig. 6a that there was a shift in the potential of the oxidation and reduction for all redox processes with the increase in scan rate. The redox pair I/I' is related to oxidation of catechol to o-quinone and its reduction to catechol, both characteristic of the system. In scan rates above 25  $\text{mV s}^{-1}$ , a new redox pair II/II' was observed (Fig. 6b), which may be related to the onset of catechol degradation. Based on voltammograms shown in Fig. 6a, one can construct the graph shown in Fig. 6c, where a linear dependence is observed for the current values recorded for both redox pairs, obtaining the linear correlation ( $R$ ) indices of  $R = 0.998$  for I,  $R = 0.996$  for I',  $R = 0.992$  for II, and  $R = 0.999$  for II'. The  $R$  values confirm that the electrochemical mechanism governing the PGE/BMNPs/CHIT/GA/PPO biosensor response is not limited by diffusion [55] and further indicate that this biosensor strongly adheres to the PGE surface [56].

**Fig. 11** Sulfite determination in industrialized juice by the standard addition method. Voltammograms obtained using PGE/BMNPs/CHIT/GA/PPO biosensor in 1.0 mM catechol solubilized in 0.1 M phosphate buffer, pH 7.2 (parameters: amp. 10 mV, freq. 20 Hz, and eq time 10 s)



### Analytical performance of the PGE/BMNPs/CHIT/GA/PPO biosensor in the presence of sulfite

To understand the effect of sulfite in the electroanalytical environment, the response of PGE/BMNPs/CHIT/GA/PPO biosensor was evaluated in the absence and presence of sulfite. The cyclic voltammograms presented in Fig. 7 show that addition of 800  $\mu\text{mol L}^{-1}$  of  $\text{SO}_3^{2-}$  reduces the current values by 70.7% for both anodic and cathodic processes. As catechol is the substrate for the PPO enzyme, the reduction peak was selected for a more detailed analytical investigation (Fig. 9). The electrochemical reaction mechanism between the biosensor and  $\text{SO}_3^{2-}$  is proposed in Fig. 8.

Sodium sulfite, as well as other sulfur compounds, has a high affinity for copper atoms in the PPO active site, leading to strong enzymatic inhibition [46]. Sulfite may inhibit PPO-driven reduction of o-quinone to catechol and/or may react with the catechol to form a catechol sulfite compound (Fig. 8) [57, 58].

The analytical performance of the biosensor was also evaluated by varying the sulfite concentration in the supporting electrolyte. These studies were carried out using a more sensitive voltammetric technique, square wave voltammetry. In Fig. 9a, it was observed that addition of sulfite to the electroanalytical medium (1.0  $\text{mmol L}^{-1}$  catechol solution in 0.1  $\text{mol L}^{-1}$  phosphate buffer) decreased the anodic peak current proportionately to the sulfite concentration, demonstrating that sulfite has an inhibitory effect on this reaction (Fig. 8).

Figure 9b shows the analytical curve obtained for the concentration range between 0 and 80  $\mu\text{M}$  sulfite, in which both the intervals  $I_1$  and  $I_2$  presented with an  $R = 0.999$ . It is observed that the slope obtained for the interval  $I_1$  was higher than that of  $I_2$ , thus showing a higher sensitivity and analytical

**Table 4** Concentration of sulfite in 3 samples of industrialized juice obtained using the PGE/MBNPs/CHIT/GA/PPO biosensor

Industrial juice sample	Sulfite concentration ( $\mu\text{M}$ )	Sulfite concentration ( $\text{mg/L}$ )
A	$8.031 \pm 0.02$	$0.643 \pm 0.02$
B	$9.102 \pm 0.01$	$0.729 \pm 0.01$
C	$3.391 \pm 0.01$	$0.271 \pm 0.01$

performance of the PGE/MBNPs/CHIT/GA/PPO biosensor for detection of sulfite at concentrations below  $30 \mu\text{M}$ . Further details on the analytical characteristics of the sensor are shown in Table 1. The limit of detection (LOD) and the limit of quantification (LOQ) were obtained from Eqs. 2 and 3, respectively [59].

$$\text{LD} = 3.3 \times \text{SD}/S \quad (2)$$

$$\text{LQ} = 10 \times \text{SD}/S \quad (3)$$

where:

SD standard deviation of the blank response;

S slope or angular coefficient of the analytical curve.

In order to show the efficiency of the sulfite biosensor developed in this work, Table 2 presents a comparative study with analytical parameters from other sulfite sensors found in literature.

Table 2 shows that the LOD for sulfite detection of PGE/MBNPs/CHIT/GA/PPO biosensor is superior only to EAu/Cyt C/SDH and GPE/IL/BF biosensors, which employ gold and graphene, among other materials of high cost. The biosensor PGE/MBNPs/CHIT/GA/PPO proposed in this work is composed of natural and low-cost polymers and is easy to prepare, thus providing an environmentally and economically viable alternative for sulfite analysis in industrial samples.

### Selectivity, sensor validation, stability, and reproducibility

Among the interferences that can be found during industrialized juice analysis, potassium sorbate, sucrose, and ascorbic acid are the most prominent. The biosensor response of PGE/MBNPs/CHIT/GA/PPO was investigated against the presence of these interferents, as shown in Fig. 10.

Potassium sorbate (Fig. 10a) and sucrose (Fig. 10b) showed no interference during the electrochemical analysis of sulfite in samples of industrialized juices, because the current remained constant even after successive additions (with increasing concentration) of these interferents.

On the other hand, after a successive addition of ascorbic acid (Fig. 10c), a slight decay in current, which was proportional to the concentration of ascorbic acid added. Therefore, this was a potential interferer in the analysis of industrialized

juices rich in vitamin C. This occurs because ascorbic acid is also a reducing agent and competes with sulfite in the enzymatic reaction between the enzyme and catechol [66].

However, it is important to note that the analytical standard addition method suppresses the effects of the analysis matrix as well as the presence of ascorbic acid in this medium, thus making this method unfeasible. Using this method, it was possible to determine the sulfite concentration in 3 samples of industrialized juices, Table 4.

The recovery of different sulfite concentrations after the enrichment of commercial juice samples was also tested (Table 3). Good recovery was obtained for most cases, and in those where the recovery percentage was above 100%, it was probably due to previously sulfite presence in the samples.

The recovery of sulfite in the juice samples demonstrates that there was no significant interference of the sample matrix in the sulfite determination by the proposed analytical procedure, demonstrating that the biosensor PGE/MBNPs/CHIT/GA/PPO is suitable for sulfite determination in samples of industrialized juices.

Additionally, the biosensor had a good stability (Fig. S1, supplementary material), which after evaluation for 30 days showed that the current levels remain constant, with only a small loss of about 7.5% in the current levels. It is important to note that the biosensor, when not in use, must remain in a refrigerator ( $4 \text{ }^\circ\text{C}$ ) and immersed in 0.1 M phosphate buffer, pH 7.2.

About reproducibility and reuse, it is important to emphasize that the biosensor PGE/MBNPs/CHIT/GA/PPO, after sulfite contact, washed and stored in ideal conditions, has its current levels restored to the initial response (when there is no sulfite), as shown in Figure S2. In this way, the electrode can be reused for several consecutive sulfite analyses.

### Indirect determination of sulfite in samples of industrialized juices

Sulfite determination was performed on three commercial juice samples (in triplicate) using the method of addition of the analytical standard, as shown in Fig. 11. The voltammograms obtained for samples B and C are shown in the supplementary material (Fig. S3 and S4). Table 3 shows the sulfite values expressed in micromolar and milligrams per liter obtained for 3 commercial juice samples.

All juice samples evaluated (Table 4) had a sulfite concentration below 10.0  $\mu\text{M}$ , within the limit established by Brazilian and international legislation.

Brazil, as well as other countries, follows the recommendations of the Joint Expert Committee on Food Additives (JECFA) on the safe use of food and beverage additives, which establishes a maximum limit of 0.02 g/100 mL sulfite in fruit juices [11, 67, 68].

The acceptable daily intake (ADI) for the use of sulfating agents in food is 0.7 mg/kg body weight/day, expressed as  $\text{SO}_2$  [69]. Similar to the FDA, the European Union has also established regulations on the acceptable limits of sulfite in food. According to the Regulation EC No. 1169/2011 (European Commission, 2011), the sulfur dioxide and sulfites in foods and beverages should not exceed 10 mg  $\text{kg}^{-1}$  (or 10 mg  $\text{L}^{-1}$ ) and are subject to mandatory labeling [70].

## Conclusions

Babaçu mesocarp nanoparticles (MBNPs), synthesized by the dialysis method, presented an irregular shape, average size around 121.5 nm, PDI 0.244, and zeta potential  $-28.1$  mV. MBNPs were used to construct the PGE/BMNP/CHIT/GA/PPO biosensor from the multilayer film adsorption onto the pyrolytic graphite carbon electrode. The electrochemical characterization of the biosensor leads us to consider it efficient for sulfite detection in industrialized juices, obtaining a detection limit of 0.151  $\mu\text{mol L}^{-1}$  and a quantitation limit of 0.452  $\mu\text{mol L}^{-1}$ . Subsequently, tests on samples of commercial juices presented sulfite concentration below 10.0  $\mu\text{M}$ , being within what is recommended by the international legislation on the guidance of the Joint Expert Committee on Food Additives which sets the maximum limit of 0.002 g/100 mL.

**Acknowledgments** The authors would like to thank the Coordination for the Improvement of Higher Education Personnel (CAPES), National Council for Scientific and Technological Development (CNPq) for the financial support received through the process 431275/2018-1 (Call MCTIC/CNPq No. 28/2018 - Universal/Range B) and the Research Productivity Grant (process 311802/2017-6 (Call CNPq No. 12/2017)). Authors also thank to Foundation for Research Support of Piauí (FAPEPI) for their financial support, and the Federal University of Piauí (UFPI) and Federal Institute of Piauí (IFPI) for providing the research and work facilities.

## Compliance with ethical standards

**Conflict of interest** The authors declare that they have no conflict of interest.

## References

- Emerton V, Choi, E (2008) Food additives and why they are used. In Essential guide to food additives. 3rd. Surrey: Leatherhead Publishing
- Saltmarsh M (2013) Essential guide to food additives, 4th edn. RSC Publishing, Cambridge
- Scampicchio M, Lawrence NS, Arecchi A, Mannino S (2008) Determination of sulfite in wine by linear sweep voltammetry. *Electroanalysis* 20:444–447
- Bahmani B, Moztarzadeh F, Rabiou M, Tahriri M (2010) Development of electrochemical sulfite biosensor by immobilization of sulfite oxidase on conducting polyaniline film. *Synth Met* 160:2653–2657
- Filik H, Çetintaş G (2012) Determination of sulfite in water and dried fruit samples by dispersive liquid-liquid microextraction combined with UV-Vis fiber optic linear array spectrophotometry. *Food Anal Methods* 5:1362–1367
- Mattison CP, Desormeaux WA, Wasserman RL, Yoshioka-Tarver M, Condon B, Grimm CC (2014) Decreased immunoglobulin E (IgE) binding to cashew allergens following sodium sulfite treatment and heating. *J Agr Food Chem* 62:6746–6755
- Suh H, Cho Y, Chung M, Kim B (2007) Preliminary data on sulfite intake from the Korean diet. *J Food Compos Anal* 20:212–219
- Iammarino M, Di Taranto M, Muscarella M (2012) Investigations on the presence of sulfites in fresh meat preparations: estimation of an allowable maximum limit. *Meat Sci* 90(2):304–308
- Vally H, Misso NLA, Madan V (2009) Clinical effects of sulfite additive. *Clin Exp Allergy* 39(11):1643–1651
- Iwasawa S, Kikuchi Y, Nishiwaki Y, Nakano M, Michikawa T, Tsuboi T, Tanaka S, Uemura T, Ishigami A, Nakashima H (2009) Effects of  $\text{SO}_2$  on respiratory system of adult Miyakejima resident 2 years after returning to the island. *J Occup Health* 51(1):38–47
- Machado RMD, Toledo MCF (2006) Sulfitos em Alimentos. *Braz J Food Technol* 9:265–275
- Stojs SJ, Miller MJS (2014) A case study involving allergic reactions to sulfur-containing compounds including, sulfite, taurine, acesulfame potassium and sulfonamides. *Food Chem Toxicol* 63: 240–243
- Dinckaya E, Sezginurk MK, Akyilmaz E, Ertaş FN (2007) Sulfite determination using sulfite oxidase biosensor based glassy carbon electrode coated with thin mercury film. *Food Chem* 101:1540–1544
- Lowinson D, Bertotti M (2001) Determination of sulfite in wine by coulometric titration. *Food Addit Contam* 18(9):773–777
- Koch M, Köppen R, Siegel D, Witt A, Nehls I (2010) Determination of total sulfite in wine by ion chromatography after in-sample oxidation. *J Agr Food Chem* 58:9463–9467
- Daunoravicius Z, Padaruskas A (2002) Capillary electrophoretic determination of thiosulfate, sulfide and sulfite using in-capillary derivatization with iodine. *Electrophoresis* 23(15):2439–2444
- Carvalho LM, Schwedt G (2005) Sulfur speciation by capillary zone electrophoresis: determination of dithionite and its decomposition products sulfite, sulfate and thiosulfate in commercial bleaching agents. *J Chromatogr A* 1099(1–2):185–190
- Satienerakul S, Phongdong P, Liawruangrath S (2010) Pervaporation flow injection analysis for the determination of sulfite in food samples utilizing potassium permanganate-rhodamine B chemiluminescence detection. *Food Chem* 121:893–898
- Amatongchai M, Sroysee W, Chairam S, Nacapricha D (2015) Simple flow injection for determination of sulfite by amperometric detection using glassy carbon electrode modified with carbon nanotubes-PDDA-gold nanoparticles. *Talanta* 133:134–141

20. Yang XF, Guo XQ, Zhao YB (2002) Novel spectrofluorimetric method for the determination of sulfite with rhodamine B hydrazide in a micellar medium. *Anal Chim Acta* 456:121–128
21. Wang C, Feng S, Wu L, Yan S, Zhong C, Guo P, Huang R, Weng X, Zhou X (2014) A new fluorescent turn-on probe for highly sensitive and selective detection of sulfite and bisulfite. *Sensors Actuat B Chem* 190:792–799
22. Chen PY, Chi YM, Yang HH, Shih Y (2012) Oil spills detection and monitoring using Airborn thermal infrared remote sensing in Dalian Xingang oil pipeline explosion. *J Electroanal Chem* 675:1–4
23. Rawal R, Chawla S, Pundir CS (2012) An electrochemical sulfite biosensor based on gold coated magnetic nanoparticles modified gold electrode. *Biosens Bioelectron* 31(1):144–150
24. Molinero-Abad B, Alonso-Lomillo MA, Domínguez-Renedo O, Arcos-Martínez MJ (2014) Sulfite oxidase biosensors based on tetrathiafulvalene modified screen-printed carbon electrodes for sulfite determination in wine. *Anal Chim Acta* 812:41–44
25. López-Gallego F, Betancor L, Mateo C, Hidalgo A, Alonso-Morales N, Dellamora-Ortiz G, Guisán JM, Fernández-Lafuente R (2005) Enzyme stabilization by glutaraldehyde crosslinking of adsorbed proteins on aminated supports. *J Biotechnol* 119(1):70–75
26. Kim J, Grate JW, Wang P (2006) Nanostructures for enzyme stabilization. *Chem Eng Sci* 61:1017–1026
27. Fiorentino D, Gallone A, Fiocco D, Palazzo G, Mallardi A (2010) Mushroom tyrosinase in polyelectrolyte multilayers as an optical biosensor for diphenols. *Biosens Bioelectron* 25(9):2033–2037
28. Falguera V, Sánchez-Riño A, Quintero-Cerón J, Rivera-Barrero C, Méndez-Arteaga J, Ibarz A (2012) Characterization of polyphenol oxidase activity in juices from 12 underutilized tropical fruits with high agroindustrial potential. *Food Bioprocess Technol* 5:2921–2927
29. Janegitz BC, Medeiros RA, Rocha-Filho RC, Fatibello-Filho O (2012) Direct electrochemistry of tyrosinase and biosensing for phenol based on gold nanoparticles electrodeposited on a boron-doped diamond electrode. *Diam Relat Mater* 25:128–133
30. Katz E, Willner I (2004) Integrated nanoparticle-biomolecule hybrid systems: synthesis, properties, and applications. *Angew Chem Int Ed* 19:6042–6108
31. Guo S, Wang E (2007) Synthesis and electrochemical applications of gold nanoparticles. *Anal Chim Acta* 598(2):181–192
32. Zhang X, Guo Q, Cui D (2009) Recent advances in nanotechnology applied to biosensors. *Sensors* 9(2):1033–1053
33. Teixeira PRS, Teixeira ASN, Farias EAO, Silva DA, Nunes LCC, Leite CMS, da Silva Filho EC, Eiras C (2018) Chemically modified babassu coconut (*Orbignya sp.*) biopolymer: characterization and development of a thin film for its application in electrochemical sensors. *J Polym Res* 25:127–138
34. Aulton ME (2005) Delineamento de formas farmacêuticas. Artmed, Porto Alegre
35. Almeida RR, Lacerda LG, Murakami FSC, Bannach G, Demiatea IM, Soccol CR, Carvalho Filho MAS, Schnitzler E (2011) Thermal analysis as a screening technique for the characterization of babassu flour and its solid fractions after acid and enzymatic hydrolysis. *Thermochim Acta* 519:50–54
36. Rao JP, Geckeler KE (2011) Polymer nanoparticles: preparation techniques and size-control parameters. *Prog Polym Sci* 36:887–913
37. Lupetti KO, Ramos LA, Fatibello-Filho O (2003) Enzymatic determination of dopamine in pharmaceutical formulations using a flow injection analysis system with avocado (*Persea americana*) crude extract. *Quim Nova* 26:197–201
38. Harper HP (1973) Manual de química fisiológica, 3rd edn. São Paulo, Atheneu Editora
39. Bradford MM (1976) Rapid and sensitive method for the quantitation of microgram quantities of protein utilizing the principle of protein-dye binding. *Anal Biochem* 72:248–254
40. Monteiro Júnior AOC, Airoidi C (1999) Some studies of crosslinking chitosan-glutaraldehyde interaction in a homogenous system. *Int J Biol Macromol* 26:119–128
41. Quintanar-Guerrero D, Allemann E, Fess IH, Doelker E (1998) Preparation techniques and mechanisms of formation of biodegradable nanoparticles from preformed polymers. *Drug Dev Ind Pharm* 24(12):1113–1128
42. Liu CH, Wu CT (2010) Optimization of nanostructured lipid carriers for lutein delivery. *Colloids Surf A Physicochem Eng Asp* 353:149–156
43. Patel VR, Agrawal YK (2011) Nanosuspension: an approach to enhance solubility of drugs. *J Adv Pharm Technol Res* 2(2):81–87
44. Zhou G, Yang JC (2004) In situ UHV-TEM investigation of the kinetics of initial stages of oxidation on the roughened Cu (110) surface. *Surf Sci* 559:100–110
45. Bhattacharjee S (2016) DLS and zeta potential – what they are and what they are not? *J Control Release* 235:337–351
46. Sartori ER, Vicentini FC, Fatibello-Filho O (2011) Indirect determination of sulfite using a polyphenol oxidase biosensor based on a glassy carbon electrode modified with multi-walled carbon nanotubes and gold nanoparticles within a poly(allylamine hydrochloride) film. *Talanta* 15:235–242
47. Vieira AP, Santana SAA, Bezerra CWB, Silva HAS, Chaves JAP, Melo JCP, da Silva Filho EC, Airoidi C (2011) Removal of textile dyes from aqueous solution by babassu coconut epicarp (*Orbignya speciosa*). *Chem Eng J* 173:334–340
48. Fráguas RM, Simão AA, Faria PV, Queiroz ER, Oliveira Junior EN, Abreu CMP (2015) Preparation and characterization chitosan edible films. *Polímeros* 25:48–56
49. Wang T, Turhan M, Gunasekaran S (2004) Selected properties of pH-sensitive, biodegradable chitosan-poly(vinyl alcohol) hydrogel. *Polym Int* 53:911–918
50. Narang J, Chauchan N, Singh A, Pundir CS (2011) A nylon membrane based amperometric biosensor for polyphenol determination. *J Mol Catal B Enzymatic* 72:276–281
51. Souza KV, Zamora PGP, Zawadzki SF (2010) Chitosan/Fe spheres on the blue QR-19 dye degradation by photo Fenton processes using artificial or solar light. *Polímeros* 20:210–214
52. Tan YY, Kan JQ, Li SQ (2011) Amperometric biosensor for catechol using electrochemical template process. *Sensor Act B Chem* 152:285–291
53. Mayer AM (2006) Polyphenol oxidases in plants and fungi: going places? A review. *Phytochemistry* 67(21):2318–2331
54. Kertesz D, Zito R (1965) Mushroom polyphenol oxidase purification and general properties. *Biochim Biophys Acta* 96:447–462
55. Xie X, Gan T, Sun D, Wu K (2008) Application of multi-walled carbon nanotubes/nafion composite film in electrochemical determination of Pb<sup>2+</sup>. *Fuller Nanotub Carbon Nanostruct* 16:103–113
56. Bard AJ, Faulkner LR (2001) Electrochemical methods fundamentals and applications. Wiley, New York
57. Namatollahi D, Tammari E, Karbasi H (2007) Electrooxidation of catechols in the presence of sulfite: presentation of a facile and green method for aromatic sulfonation. *Int J Electrochem Sci* 2:986–995
58. Goto Y, Matsui T, Ozaki S-I, Watanabe Y, Fukuzumi S (1999) Mechanisms of sulfoxidation catalyzed by high-valent intermediates of heme enzymes: electron-transfer vs oxygen-transfer mechanism. *J Am Chem Soc* 121:9497–9502
59. Anvisa (2003) Resolução RDC no. 899, de 29 de maio de 2003. Ministério da Saúde - MS. Agência Nacional de Vigilância Sanitária – Anvisa

60. Rawal R, Pundir CS (2013) Development of electrochemical sulfite biosensor based on SOx/PBNPs/PPY modified Au electrode. *Biochem Eng J* 71:30–37
61. Ameer Q, Adeloju SB (2008) Galvanostatic entrapment of sulfite oxidase into ultrathin polypyrrole films for improved amperometric biosensing of sulfite. *Electroanalysis* 20:2549–2556
62. Kalimuthu P, Tkac J, Kappler U, Davis JJ, Bernhardt PV (2010) Highly sensitive and stable electrochemical sulfite biosensor incorporating a bacterial sulfite dehydrogenase. *Anal Chem* 82(17): 7374–7379
63. Abass AK, Hart JP, Cowell D (2000) Development of an amperometric sulfite biosensor based on sulfite oxidase with cytochrome c, as electron acceptor, and a screen-printed transducer. *SensorActuat B* 62:148–153
64. Beitollahi H, Tajik S, Biparva P (2014) Electrochemical determination of sulfite and phenol using a carbon paste electrode modified with ionic liquids and graphene nanosheets: application to determination of sulfite and phenol in real samples. *Measurement* 56:170–177
65. Rawal R, Chawla S, Dahiya T, Pundir CS (2011) Development of an amperometric sulfite biosensor based on a gold nanoparticles/chitosan/multiwalled carbon nanotubes/polyaniline-modified gold electrode. *Anal Bioanal Chem* 401(8):2599–2608
66. Fatibelo Filho O, Vieira IC (1997) Flow injection spectrophotometric determination of sulfite using a crude extract of sweet potato root (*Ipomoea batatas* (L.) Lam.) as a source of polyphenol oxidase. *Anal Chim Acta* 354:51–57
67. Brasil. Agência Nacional de Vigilância Sanitária (1997) Portaria no. 540 – SVS/MS de 27 de outubro de 1997. Aprova o Regulamento Técnico: Aditivos Alimentares - definições, classificação e emprego [acesso em 3 maio 2019]. Disponível em: [http://www.anvisa.gov.br/legis/portarias/540\\_97.htm](http://www.anvisa.gov.br/legis/portarias/540_97.htm)
68. ABIA (2001) – Associação Brasileira das Indústrias da Alimentação. *Compêndio da Legislação Brasileira de Alimentos*, seção 3.31
69. FAO/WHO (2007) Summary of evaluations performed by the Joint FAO/WHO Expert Committee on Food Additives. Sulfur dioxide. Food and Agriculture Organization/World Health Organization, Rome, Italy and Geneva, Switzerland
70. European Commission (2011) Council Regulation of 25 October 2011 on the provision of food information to consumers, amending Regulations (EC) No 1924/2006 and (EC) No 1925/2006 of the European Parliament and of the Council, and repealing Commission Directive 87/250/EEC, Council Directive 90/496/EEC, Commission Directive 1999/10/EC, Directive 2000/13/EC of the European Parliament and of the Council, Commission Directives 2002/67/EC and 2008/5/EC and Commission Regulation (EC) N. 608/2004, 1169/2011/EC. In: *Official Journal*, L 304/18, 22.11.2011

**Publisher's note** Springer Nature remains neutral with regard to jurisdictional claims in published maps and institutional affiliations.